Watt-level Flat Supercontinuum Source Pumped by Noise-like Pulse from an All-fiber Oscillator

He Chen, Shengping Chen, Zongfu Jiang and Jing Hou
College of Optoelectronic Science and Engineering, National University of Defense Technology, Changsha 410073, China
chenhhe@qq.com, chespn@163.com, jingzongfu7@163.com, houjing25@sina.com

Keywords: Supercontinuum Generation, Ultrafast Optics, Mode-locked Lasers, Fiber Lasers.

Abstract: We demonstrate Watt-level flat visible supercontinuum (SC) generation in photonic crystal fibers, which is directly pumped by broadband noise-like pulses from an Yb-doped all-fiber oscillator. The novel SC generator is featured with elegant all-fiber-integrated architecture, high spectral flatness and high efficiency. Wide optical spectrum spanning from 500 nm to 2300 nm with 1.02 W optical power is obtained under the pump power of 1.40 W. The flatness of the spectrum in the range of 700 nm~1600 nm is less than 5 dB (including the pump residue). The exceptional simplicity, economical efficiency and the comparable performances make the noise-like pulse oscillator a competitive candidate to the widely used cascade amplified coherent pulse as the pump source of broadband SC. To the best of our knowledge, this is the first demonstration of SC generation which is directly pumped by an all-fiber noise-like pulse oscillator.

1 INTRODUCTION

The phenomenon of supercontinuum (SC) generation in nonlinear medium, especially in optical fibers, is appreciated as one of the most spectacular in nonlinear physics. Owing to the unique combination of extremely broad spectral bandwidths, high spectral power densities, and high spatial coherence, fiber-based supercontinuum lasers have found numerous applications in areas such as spectroscopy and microscopy (Dudley et al., 2006).

There are two critical requisites for SC generation, the first one is the nonlinear medium, including various bulk materials and nonlinear optical fibers, among which photonic crystal fiber (PCF) had attracted the most intensive attentions because of its unprecedented design freedom of the dispersion properties (Russell, 2003, Knight et al., 2000). Specifically, by design optimization of the zero dispersion wavelength (ZDW), SC covering the whole visible spectrum can be facilely generated from fibers (Stone and Knight, 2008).

Beside the nonlinear medium, highly intensive pump source plays another essential role in process of the broadband SC generation. In terms of the temporal durations of the pump pulses, there are typically three commonly used pumping schemes, which are pumping with fs pulse (Ranka et al., 2000), ps-ns long pulse (Coen et al., 2001, Xiong et al., 2006, Chen et al., 2011a, Chen et al., 2013) and continuous wave (CW)/quasi-CW (Travers et al., 2008, Cumberland et al., 2008), respectively. Each kind of pump lasers evolve in partially different way in the nonlinear medium, especially when they are launched in the abnormal dispersion region.

Beside those three typical types of pump lasers, there is another intriguing optical pulse form, called noise-like pulse (NLP) or double-scale pulse (Horowitz et al., 1997, Tang et al., 2005a, Zhao et al., 2007, Kobtsev et al., 2009, Yu et al., 2014, Churkin et al., 2015, Liu et al., 2015), which has been recently widely investigated and was also exploited as the pump source to achieve spectral broadening and nonlinear frequency generation in nonlinear medium (Zaytsev et al., 2013, Kobtsev et al., 2014, Lin et al., 2014, Runge et al., 2014, Smirnov et al., 2014, You et al., 2015). NLP is quite distinct from those standard mode-locked pulses in two ways. Temporally, NLP is regarded as stochastic fs bunch localized in a ps-ns pulse packet. Spectrally, it is featured with the ultra-broadband spectrum, which is actually the superposition of incoherent single pulses' spectra (Runge et al., 2013). Although the "unstable" nature usually makes NLP regarded to own limited practical usability because of its intractability, interestingly, pumping nonlinear medium with NLP had shown several advantages over similar single pulse sequence. For example, it had been experimentally shown that double-scale pulses manifest more efficient Raman transformation comparing with single scale pulses, leading to broader supercontinuum spectra (Kobtsev et al., 2014). And similar conclusion was also drawn in the scenarios of second-harmonic generation with NLP (Smirnov et al., 2014).

Actually NLP-pumped SC generation has been recently investigated in several kinds of nonlinear fibers, such as standard SMF-28 (Zaytsev et al., 2013), highly nonlinear fiber (Lin et al., 2014), P2O5-doped fiber (Kobtsev et al., 2014), and widely extended spectra have been obtained, however none of them extended to visible spectral regions, which is mainly restricted by the dispersion properties of the used nonlinear fibers. Moreover, in all of the related investigations, at least one stage of fiber amplifier was included in the configuration to boost the pump power.

In this manuscript, we report a novel elegant scheme of Watt-level visible SC generation which takes advantages both of the unique dispersion properties of PCF and the special features of NLP. Firstly, unlike fore-reported investigations on NLP-pumped near-infrared SC generation, we use PCF to expand the spectrum to both visible and infrared directions. Secondly, no fiber amplifier is used in the configuration, the SC is directly pumped by the NLP from an ultra-simple all-fiber master oscillator, by which the whole system is much more compact comparing with its counterparts. Actually the work is partially motivated by simplifying the architecture of SC source. By significantly reducing the complexity, and the cost of SC laser sources, Watt-level pocket SC source will be possible and applications within new areas can be enabled. Besides, the differences in the mechanisms between NLP-pumped SC generation and regular-pulse-pumped one are discussed.

2 EXPERIMENTAL SETUP

The architecture of the all-fiber-integrated supercontinuum generator is depicted in Fig.1, which is constructed with an ultra-simple mode-locked Yb-doped all-fiber oscillator and a section of PCF. The Yb-doped fiber oscillator is formed with two NOLMs and a cladding-pumped fiber amplifier. The left NOLM was made by a 50:50 fused coupler and a section of 35-meters-long twisted passive fiber in the loop. The right NOLM was made by a 10:90 fused coupler. Both of the NOLMs act as the reflective mirrors of the oscillator for laser oscillating and artificial saturable absorber for mode-locking simultaneously. Two fiber-squeezer-based polarization controllers were applied on both of the NOLMs to control their nonlinear reflection characteristics, which are essential for manipulating the mode-locking behaviors (Chen et al., In press). The fiber amplifier is formed with a section of double-cladding 10/125 Yb-doped fiber, a 976 nm multimode laser diode as the pump source, and a pump/signal combiner.

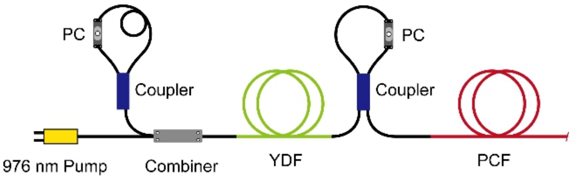

Figure 1: The schematic of the proposed supercontinuum generator. PC: polarization controller; YDF: Yb-doped fiber; PCF: photonic crystal fiber.

By proper polarization controlling, the fiber oscillator before the PCF can be operated in the NLP regime, where the pulse peak power can be increased almost linearly with the pump power. The repetition rate was measured to be 3.52 MHz by an oscilloscope. Under the pump power of 5.8 W, the highest power energy of 0.4 μJ and average peak power of 7 kW were obtained. The corresponding autocorrelator trace has a short 100-fs-wide peak and a 57-ps-wide pedestal beneath it, which reveals the noise-like nature of the output pulses: the pulse is actually a pulse packet rather than an integrated single pulse, which is formed with stochastic 100-fs inner pulse. The output spectrum has a 3 dB spectral width of 76 nm. The detailed characteristics of the pump oscillator can be found in our previous contribution (Chen et al., In press). Notably, it is believed that stimulated Raman scattering (SRS) plays an essential role in the formation of the NLP and its ultra-broadband spectrum (Aguergaray et al., 2013, Tang et al., 2005a).

Two sections of solid core PCFs were employed in the experiment as the main nonlinear spectral broadening medium. The first one has a core diameter of 4.7 μm with 6-layers of hexagonal air holes arranged in the cladding. The second one has similar structure, but a larger core diameter of 7.5 μm. The cross profiles of the two PCFs are shown as in Fig. 3. The calculated dispersion curves of the PCFs are also illustrated in Fig. 3. As we can see, the two PCFs have different zero-dispersion-wavelengths (ZDWs) of 1035 nm and 1118 nm respectively. We use "PCF 1" and "PCF 2" to refer to the two PCF respectively. The 3 dB spectral bandwidth of the pumping NLP ranges from 1070 nm to 1146 nm, which is totally in the abnormal dispersion region of PCF 1, and partially normal/ partially abnormal dispersion region of PCF 2. The PCF and the 10/125 output fiber were fusion spliced with the technique of controlled hole collapse to reduce the splicing loss (Chen et al., 2011b), which is estimated to be around 0.5 dB.

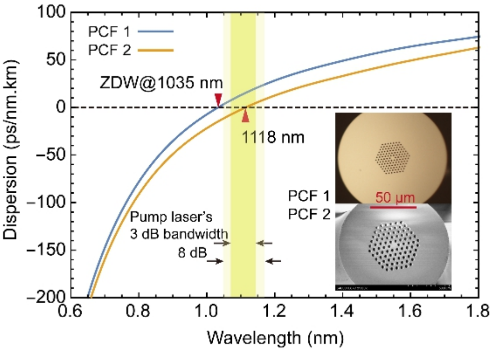

Figure 2: The calculated dispersion curves and the cross profiles of PCF 1 and PCF 2.

3 EXPERIMENTAL RESULTS AND DISCUSSIONS

By propagating through a 3-meters-long PCF 1, the spectrum of the output pulse was significantly expanded. Figure 4 shows the evolution of the generated SC the different pump power levels. The spectra in the range of 400 nm-1200 nm and 1200 nm-2400 nm were separately measured by two different optical spectrum analyzers with the same spectral resolution of 0.5 nm, and were joined together in Fig. 4. A 1400 nm cut-on long pass filter was employed after the output port when measuring the spectra of 1400 nm-2400 nm to avoid the second order harmonics of 700 nm-1200 nm spectra. The SC was delivered to the optical spectrum analyzers through a short section of multimode fiber, and the high order mode interference in the delivering fiber caused the fine fluctuations on the spectral curves.

As the pump power increased from 0.5 W to 1.4 W, the spectrum expanded towards both of the long and the short wavelength directions simultaneously, as exhibited in Fig. 4. Under the highest pump power of 1.4 W, a wide and flat SC spectrum with total power of 1.02 W is obtained which spans over 1800 nm, ranging from ~500 nm to ~2300 nm. The spectrum has excellent flatness in a large spectral range. Unlike the traditional ps-pulse-pumped SC with a high pump residue peak on the spectrum, in this case, the broadband pump residue was merged with the extended spectral components, forming an integrated and super-flat SC. The 6 dB spectral bandwidth spanned from 685 nm to 1620 nm, and 20 dB bandwidth spanned from 540 nm to 2040 nm (including the pump residue).

The spectral flatness and smoothness as exhibited in this NLP-pumped SC were regarded as the typical feature and one of the great benefits of ps-ns long pulse pumped SC, which indicated that there is similar mechanism underlying the two different pumping scheme. It is reasonable in a qualitative perspective. For the case of SC generation pumped with ps-ns long pulse in the abnormal dispersion region, modulation instability (MI) causes the temporal breakup of the long input pulse and transform them into a bunch of numerous stochastic fs-level solitons in the initial phase before the dramatic spectral extending (Dudley et al., 2009). The MI-induced incoherent soliton bunch, to some extent, resembles the characteristics of the incoherent NLP, which is also regarded as a bunch of fs-level stochastic sub-pulses, and those sub-pulses will be further broken down to narrower solitons after the process of pulse compression and soliton fission. Although the initial evolution process of the two kinds of pumping pulses in PCF may be different, the outcomes are similar, both of which evolve to a great bunch of stochastic solitons, except that the distributions of the solitons' pulse duration and peak power may differ from each other. However, the exact differences between the MI-induced soliton bunch and the NLP formed in the mode-locking oscillator requires specific numerical and experimental investigation.

After the process of solitons formation, the spectra are dramatically extended driven by the soliton dynamics, where the Raman induce soliton self-frequency shift (SSFS) is mainly responsible for the generation of long wavelength spectra, and the spectral extension towards the short-wavelength-side is driven by the corresponding dispersive wave generation in the normal dispersion region. While the soliton is being red-shifted due to SSFS, it traps a packet of dispersive waves under the group-velocity matched condition, which is called soliton trapping of dispersive waves, so that the dispersive waves are further blue-shifted resulting the group velocity matching of the spectral edges (Gorbach and Skryabin, 2007). The spectrum exhibits a continuous broadening towards both sides of the pump wavelength in this process. The spectrum should be further expanded to both of the red and blue sides by increasing the pump power.

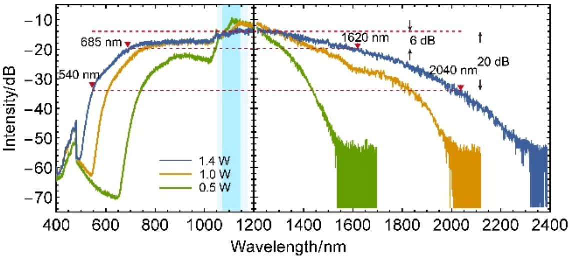

Figure 3: The spectral evolution process of the generated SC in PCF 1 under the different pump power levels.

Different from pumping PCF 1 in the abnormal dispersion region, in this section, we exhibit the experimental results of simultaneously pumping in the normal and abnormal dispersion region of PCF 2, whose ZDW is at 1118 nm. As we can see in Fig. 3, the center wavelength of the broadband pumping NLP is located very close to the ZDW of PCF 2, nearly half of the pump lay in the normal dispersion region, and the other half in the abnormal region. The length of PCF 2 used in the experiment is 6 m, as it has relatively large effective mode area and low nonlinear parameter, it is elongated to sufficiently enhance the fiber nonlinearities. Figure 5 shows the evolution process of the generated SC under different pump power levels. As we can see, the bandwidth of the SC from PCF 2 at the same pump power is much narrower than the one from PCF 1, especially at the pump power of 0.5 W and 1.0 W. However, under the pump power of 1.4 W, the generated SC spans over more than 1750 nm, ranging from 550 nm to 2300 nm, with the total power of 1.05 W, which is similar with the case of PCF 1, except that the short wavelength edge ceased at 550 nm rather than 500 nm in PCF 1. The difference in the short wavelength edges is mainly determined by the different group velocity matching curves of the two PCFs. Although nearly half of the pump is located at the normal dispersion region of the PCF, the generated SC shows similar characteristics with the case of all abnormal dispersion pumping.

The NLP-pumped SC generated in PCF 1 and PCF 2 shown in the previous two sections have manifested that NLP can be used to generating flat and broadband SC even with a relatively low pump power without any additional amplifiers. These experimental results make essential contributions to the subject of SC generation in two aspects.

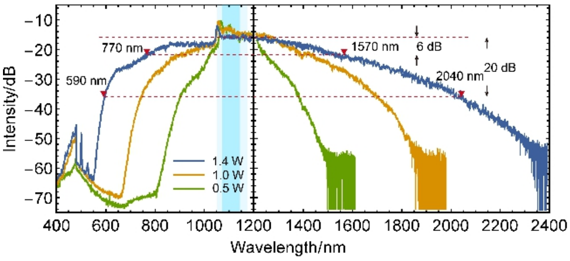

Figure 4: The spectral evolution process of the generated SC in PCF 2 under the different pump power levels.

The first one is that this NLP-pumped SC generation scheme can be of great practical utility because of its structural simplicity and the comparable performances. Actually, it is a trait of NLP that it can be generated directly from mode-locked fiber oscillator with high pulse energy and peak power. While, regular single pulse, like soliton and dissipative soliton, which are directly produced from all-fiber oscillator, always have limitations in peak power and pulse energy scalability. Pulse splitting or harmonic mode locking can be induced by the peak power clamping effect under intensive pump power (Tang et al., 2005b, Liu, 2010), resulting a limitation in the output peak power, which is critical for broadband SC generation. Hence, traditional regular pulse pumped all-fiber SC laser source always involves cascaded fiber amplifiers. As an instance, the dual-NOLM-based mode-locked fiber laser used in the experiment can also produce single pulse sequence in the dissipative soliton and dissipative soliton resonance regime by polarization controlling (Chen et al., In press), but in both regimes, the output peak powers are all limited below 1 kW. The special facility of generating pulses (packets) with high peak power directly from fiber oscillator under intensive pump power was also verified numerically (Knight et al., 2000). Hence, for the applications where the coherence of SC is not a requisition, the employment of intensively pumped all-fiber NLP oscillator as the pump source of SC generation is feasible and a much more economically efficient and simplified scheme, comparing with the traditional cascaded-amplifier-based one. We believe, by further improving the stability and robustness, this scheme may make Watt-level pocket SC source possible, from which a great many of applications could benefit. Even for applications where highly powerful all-fiber SC generation is required, the employment of high power NLP fiber oscillator as the seed laser of the cascaded fiber amplifiers will save one or two stages of pre-amplifiers.

Beside the practical utility, there are also scientific subjects involved in the physical process of the NLP-pumped SC generation. As mentioned before, the distinct temporal structure of incoherent NLP makes the initial evolution process of NLP-pumped SC generation different with the scenarios of pumping with coherently mode-locked ps-ns long pulses in abnormal dispersion region. Briefly speaking, coherently mode-locked long pulses evolve to incoherent soliton bunch under the influence of MI, while NLP itself is incoherent soliton-resembling bunch with stochastic sub-pulse durations and peak powers. In other words, as a qualitative description, the primary place where the process of pulse breakup happens is different in the two pumping schemes, one is in the mode-locking oscillator under the main influence of SRS (Runge et al., 2014, Aguergaray et al., 2013), while the other is in the PCF under the influence of MI. As NLP often owns diversified temporal and spectral structures, which may involves complex processes like the generation of optical rogue waves, there may be some possibilities to manipulate the SC generation by engineering the formation of NLP in the pumping fiber oscillator. To answer those remaining questions and verify the speculations, a theoretical framework which incorporates both of the NLP dynamics and the SC generation dynamics will be built in future investigations.

It should be noted that the PCFs used in the experiments are all commercial fibers without specific dispersion engineering. We believe this ultra-compact SC generation scheme with all-fiber NLP oscillator as the pump can be further developed towards higher output power and wider spectrum extending to violet region by the employment of specifically designed PCF and the optimization of the pumping oscillator.

4 CONCLUSIONS

We demonstrate Watt-level flat visible SC generation in PCFs, which is directly pumped by broadband noise-like pulses from an Yb-doped all-fiber oscillator. Two different PCFs were tested. In PCF 1, wide optical spectrum spanning from 500 nm to 2300 nm with 1.02 W optical power is obtained under the pump power of 1.40 W. The flatness of the spectrum in the range of 700 nm~1600 nm is less than 5 dB (including the pump residue). The largely simplified architecture, exceptional flatness, and provide another feasible to the commonly used scheme with single pulse sequence as the pump. We believe the spectrum bandwidth and output power can be further elevated by PCF optimizing the cavity design of the pump oscillator and characteristics of the NLP. With very limited amount of optical components, it is probably the most economically efficient watt-level visible SC source ever. By reducing the complexity and the cost of Watt-level visible SC laser sources, applications within new areas can be enabled.

REFERENCES

Aguergaray, C., Runge, A., Erkintalo, M. & Broderick, N. G. R. 2013. Raman-driven destabilization of mode-locked long cavity fiber lasers: fundamental limitations to energy scalability. Optics Letters, 38, 2644-2646.

Chen, H., Chen, S., Jiang, Z. & Hou, J. In press. 0.4 μJ, 7 kW ultra-broadband noise-like pulse direct generation from an all-fiber dumbbell-shaped laser. Opt. Lett.

Chen, H., Chen, S., Wang, J., Chen, Z. & Hou, J. 2011a. 35W high power all fiber supercontinuum generation in *PCF with picosecond MOPA laser. Optics Communications*, 284, 5484-5487.

Chen, H., Chen, Z., Chen, S., Hou, J. & Lu, Q. 2013. Hundred-watt-level, all-fiber-integrated supercontinuum generation from photonic crystal fiber. *Applied Physics Express*, 6, 032702.

Chen, Z., Xi, X., Zhang, W., Hou, J. & Jiang, Z. 2011b. Low-loss fusion splicing photonic crystal fibers and double cladding fibers by controlled hole collapse and tapering. *Lightwave Technology, Journal of*, 29, 3744-3747.

Cheng, Z., Li, H. & Wang, P. 2015. Simulation of generation of dissipative soliton, dissipative soliton resonance and noise-like pulse in Yb-doped mode-locked fiber lasers. Optics Express, 23, 5972-5981.

Churkin, D. V., Sugavanam, S., Tarasov, N., Khorev, S., Smirnov, S. V., Kobtsev, S. M. & Turitsyn, S. K. 2015. Stochasticity, periodicity and localized light structures in partially mode-locked fibre lasers. Nat Commun, 6, 7004.

Coen, S., Chau, A. H. L., Leonhardt, R., Harvey, J. D., Knight, J. C., Wadsworth, W. J. & Russell, P. S. J. 2001. White-light supercontinuum generation with 60-ps pump pulses in a photonic crystal fiber. *Optics Letters,* 26, 1356-1358.

Cumberland, B. A., Travers, J. C., Popov, S. V. & Taylor, J. R. 2008. Toward visible cw-pumped supercontinua. Optics Letters, 33, 2122-2124.

Dudley, J. M., Genty, G. & Coen, S. 2006. Supercontinuum generation in *photonic crystal fiber. Reviews of Modern Physics*, 78, 1135-1184.

Dudley, J. M., Genty, G., Dias, F., Kibler, B. & Akhmediev, N. 2009. Modulation instability, Akhmediev Breathers and continuous wave supercontinuum generation. *Optics express*, 17, 21497-21508.

Gorbach, A. V. & Skryabin, D. V. 2007. Light trapping in gravity-like potentials and expansion of supercontinuum spectra in *photonic-crystal fibres. Nature Photonics*, 1, 653-657.

Horowitz, M., Barad, Y. & Silberberg, Y. 1997. Noiselike pulses with a broadband spectrum generated from an erbium-doped fiber laser. *Optics letters*, 22, 799-801.

Knight, J., Arriaga, J., Birks, T., Ortigosa-Blanch, A., Wadsworth, W. & Russell, P. S. J. 2000. Anomalous dispersion in photonic crystal fiber. *Photonics Technology Letters, IEEE*, 12, 807-809.

Kobtsev, S., Kukarin, S., Smirnov, S. & Ankudinov, I. 2014. Cascaded SRS of single- and double-scale fiber laser pulses in long extra-cavity fiber. *Optics Express*, 22, 20770-20775.

Kobtsev, S., Kukarin, S., Smirnov, S., Turitsyn, S. & Latkin, A. 2009. Generation of double-scale femto/pico-second optical lumps in mode-locked fiber lasers. *Optics Express*, 17, 20707-20713.

Lin, S.-S., Hwang, S.-K. & Liu, J.-M. 2014. Supercontinuum generation in highly nonlinear fibers using amplified noise-like optical pulses. *Optics Express*, 22, 4152-4160.

Liu, J., Chen, Y., Tang, P., Xu, C., Zhao, C., Zhang, H. & Wen, S. 2015. Generation and evolution of mode-locked noise-like square-wave pulses in a large-anomalous-dispersion Er-doped ring fiber laser. *Optics Express*, 23, 6418-6427.

Liu, X. 2010. Hysteresis phenomena and multipulse formation of a dissipative system in a passively mode-locked fiber laser. *Physical Review A*, 81, 023811.

Ranka, J. K., Windeler, R. S. & Stentz, A. J. 2000. Visible continuum generation in air-silica microstructure optical fibers with anomalous dispersion at 800 nm. Opt. Lett., 25, 25-27.

Runge, A. F. J., Aguergaray, C., Broderick, N. G. R. & Erkintalo, M. 2013. Coherence and shot-to-shot spectral fluctuations in noise-like ultrafast fiber lasers. *Optics Letters*, 38, 4327-4330.

Runge, A. F. J., Aguergaray, C., Broderick, N. G. R. & Erkintalo, M. 2014. Raman rogue waves in a partially mode-locked fiber laser. *Optics Letters*, 39, 319-322.

Russell, P. 2003. Photonic Crystal Fibers. Science, 299, 358-362.

Smirnov, S. V., Kobtsev, S. M. & Kukarin, S. V. 2014. Efficiency of non-linear frequency conversion of double-scale pico-femtosecond pulses of passively mode-locked fiber laser. *Optics Express*, 22, 1058-1064.

Stone, J. M. & Knight, J. C. 2008. Visibly "white" light generation in uniform photonic crystal fiber using a microchip laser. *Optics Express*, 16, 2670-2675.

Tang, D., Zhao, L. & Zhao, B. 2005a. Soliton collapse and bunched noise-like pulse generation in a passively mode-locked fiber ring laser. *Optics express*, 13, 2289-2294.

Tang, D., Zhao, L., Zhao, B. & Liu, A. 2005b. Mechanism of multisoliton formation and soliton energy quantization in passively mode-locked fiber lasers. *Physical Review A*, 72, 043816.

Travers, J. C., Rulkov, A. B., Cumberland, B. A., Popov, S. V. & Taylor, J. R. 2008. Visible supercontinuum generation in photonic crystal fibers with a 400W continuous wave fiber laser. *Optics Express*, 16, 14435-14447.

Xiong, C., Witkowska, A., Leon-Saval, S. G., Birks, T. A. & Wadsworth, W. J. 2006. Enhanced visible continuum generation from a microchip 1064nm laser. *Optics Express*, 14, 6188-6193.

You, Y.-J., Wang, C., Xue, P., Zaytsev, A. & Pan, C.-L. Supercontinuum Generated by Noise-like Pulses for Spectral-domain Optical Coherence Tomography. CLEO: 2015, 2015/05/10 2015 San Jose, California. *Optical Society of America*, JW2A.94.

Yu, C., Man, W., Pinghua, T., Shuqing, C., Juan, D., Guobao, J., Ying, L., Chujun, Z., Han, Z. & Shuangchun, W. 2014. The formation of various multi-soliton patterns and noise-like pulse in a fiber laser passively mode-locked by a topological insulator based saturable absorber. *Laser Physics Letters*, 11, 055101.

Zaytsev, A., Lin, C.-H., You, Y.-J., Chung, C.-C., Wang, C.-L. & Pan, C.-L. 2013. Supercontinuum generation by noise-like pulses transmitted through normally dispersive standard single-mode fibers. *Optics Express*, 21, 16056-16062.

Zhao, L. M., Tang, D. Y., Wu, J., Fu, X. Q. & Wen, S. C. 2007. Noise-like pulse in a gain-guided soliton fiber laser. *Optics Express*, 15, 2145-2150.